

This is the accepted manuscript made available via CHORUS. The article has been published as:

Reducing microwave absorption with fast frequency modulation

Juehang Qin and A. Hubler

Phys. Rev. E **95**, 052201 — Published 2 May 2017

DOI: [10.1103/PhysRevE.95.052201](https://doi.org/10.1103/PhysRevE.95.052201)

Reducing Microwave Absorption with Fast Frequency Modulation

Juehang Qin, A. Hubler

UIUC

(Dated: April 7, 2017)

Abstract

We study the response of a two-level quantum system to a chirp signal, using both numerical and analytical methods. The numerical method is based on numerical solutions of the Schrödinger solution of the two-level system, while the analytical method is based on an approximate solution of the same equations. We find that when two-level systems are perturbed by a chirp signal, the peak population of the initially unpopulated state exhibits a high sensitivity to frequency modulation rate. We also find that the aforementioned sensitivity depends on the strength of the forcing, and weaker forcings result in a higher sensitivity, where the frequency modulation rate required to produce the same reduction in peak population would be lower. We discuss potential applications of this result in the field of microwave power transmission, as it shows applying fast frequency modulation to transmitted microwaves used for power transmission could decrease unintended absorption of microwaves by organic tissue.

I. INTRODUCTION

Wireless power transfer is currently an active area of research, with multiple technologies being pursued and evaluated. Xie *et al.*[1] classified the various methods currently in use or in development into four categories, which are inductive coupling, omnidirectional electromagnetic radiation, unidirectional electromagnetic radiation, and magnetic resonance coupling. They also described the advantages and disadvantages of various methods. Inductive coupling has high power efficiency and is simple to implement, however is limited to very close range, where the transmission distance is on the order of the size of the inductive coil. Magnetic resonance coupling provides greater range, up to several meters, however has more complexity than inductive coupling. Omnidirectional radiation provides the advantage of allowing very small receivers, however suffers from inverse square dropoff over distance, impacting efficiency. Directed radiation provides high efficiency and range, however requires line of sight and tracking mechanisms for mobile targets.

Power transfer by directed radiation can be further classified into two types, microwave transmission and optical transmission, though functionally, the distinction is becoming less significant due to the recent development of optical rectenna technology [2]. Optical power transmission using lasers has the main advantage of allowing much smaller apertures for both the transmitter and the receiver, however is plagued by attenuation from weather effects [3]. With microwaves, high energy densities are routinely achieved resonant cavities and waveguides, such as within microwave ovens. In addition, microwave power transfer can achieve a high efficiency, with realized rectenna efficiencies of above 80% [4]. However, outside of a confined waveguide or cavity, intense microwave radiation can be harmful to living beings [5]. These safety concerns are one of the few final issues delaying commercial deployment of microwave power transfer [6]. Sinusoidal microwaves are most effective in transferring energy to matter or to a linear microwave antenna, because the dynamics of both systems is linear; quantum systems are described by the linear Schrödinger equation and conventional antenna are linear oscillators. The above effects also imply that it is difficult to transmit microwaves through dense media [7]. This has implications for communications with and supplying power to underwater craft and embedded sensors, such as medical sensors inside the human body.

We show that the absorption of frequency modulated microwaves by matter is much

less, because fast frequency modulation of microwaves results in decreased resonance of quantum systems. This suggests that most dielectric and poorly conducting matter is largely transparent to frequency modulated microwaves, including organic materials and water. Despite that, it is known that nonlinear systems captured into resonance can continue to resonate even as the forcing frequency is modulated [8], suggesting frequency modulated microwaves can resonate with nonlinear antennas. This implies that frequency modulated microwaves can pass undiminished through matter, and then be absorbed by a nonlinear antenna, and thereby transport energy from an energy source to an energy sink, while minimizing energy absorption by other sources. We discuss potential applications for safe and secure wireless power transfer.

II. DESCRIPTION OF TWO LEVEL QUANTUM SYSTEM

We consider a system with two base states, $|1\rangle$ and $|2\rangle$, where the two base states are symmetric, such as in the case of an ammonia molecule with spin states Up or Down. The state vector of that system would then be defined by Equation (1).

$$|\psi\rangle = C_1|1\rangle + C_2|2\rangle \quad (1)$$

The Hamiltonian can be expressed as Equation (2), when there is an external time-dependent field. μ represents the dipole moment, and $\mathcal{E}(t)$ represents the time-varying field.

$$H_0 = \begin{pmatrix} E_0 + \mu\mathcal{E}(t) & -A \\ -A & E_0 - \mu\mathcal{E}(t) \end{pmatrix} \quad (2)$$

The Hamiltonian in Equation (2) can be transformed into Equation (3).

$$H = \begin{pmatrix} E_0 + A & \mu\mathcal{E}(t) \\ \mu\mathcal{E}(t) & E_0 - A \end{pmatrix} \quad (3)$$

The transformation matrix is as shown in Equation (4).

$$S = \frac{1}{\sqrt{2}} \begin{pmatrix} 1 & -1 \\ 1 & 1 \end{pmatrix} \quad (4)$$

The Hamiltonian H shown in Equation (3) is useful as it represents the diagonalized Hamiltonian if there is no external field, and can be considered almost diagonal for weak

fields. The basis states based on this Hamiltonian is shown in Equation (5).

$$|\psi\rangle = C_I|I\rangle + C_{II}|II\rangle \quad (5)$$

This yields the system of differential equations shown in Equation (6).

$$\begin{aligned} i\hbar \frac{dC_I}{dt} &= (E_0 + A)C_I + \mu\mathcal{E}(t)C_{II}, \\ i\hbar \frac{dC_{II}}{dt} &= (E_0 - A)C_{II} + \mu\mathcal{E}(t)C_I \end{aligned} \quad (6)$$

In the case of a electric field that is weak, such that $\mu\mathcal{E} \ll A$, C_I and C_{II} can be expressed as per Equation (7).

$$\begin{aligned} C_I &= \gamma_I e^{-i(E_0+A)t/\hbar} \\ C_{II} &= \gamma_{II} e^{-i(E_0-A)t/\hbar} \end{aligned} \quad (7)$$

The system described in Equation (6) can then be formulated as Equation (8).

$$\begin{aligned} i\hbar \frac{d\gamma_I}{dt} &= \mu\mathcal{E}(t)e^{i\omega_0 t}\gamma_{II}, \\ i\hbar \frac{d\gamma_{II}}{dt} &= \mu\mathcal{E}(t)e^{-i\omega_0 t}\gamma_I \end{aligned} \quad (8)$$

where $\hbar\omega_0 = 2A$.

Such a system can be pertubed by an electric field defined by Equation (9). This can be a good approximation for a planar electromagnetic wave with varying frequency, as long as wavelength is significantly longer than the system concerned, such that the gradient of the field is not significant.

$$\mathcal{E} = 2\mathcal{E}_0 \cos((\omega_0 + \Delta(t))t) \quad (9)$$

In that case, Equation (8) can be expressed as Equation (10).

$$\begin{aligned} i\hbar \frac{d\gamma_I}{dt} &= \mu\mathcal{E}_0 [e^{i(2\omega_0+\Delta(t))t} + e^{-i\Delta(t)t}] \gamma_{II}, \\ i\hbar \frac{d\gamma_{II}}{dt} &= \mu\mathcal{E}_0 [e^{i\Delta(t)t} + e^{-i(2\omega_0+\Delta(t))t}] \gamma_I \end{aligned} \quad (10)$$

For small values of μE_0 , $\frac{d\gamma_I}{dt}$ and $\frac{d\gamma_{II}}{dt}$ are small. Hence, it is a reasonable approximation to take $e^{\pm i(2\omega_0+\Delta(t))t} = 0$, as 0 is the average value of the oscillation. This approximation, known as the rotating wave approximation, yields Equation (11).

$$\begin{aligned} i\hbar \frac{d\gamma_I}{dt} &= \mu\mathcal{E}_0 e^{-i\Delta(t)t} \gamma_{II}, \\ i\hbar \frac{d\gamma_{II}}{dt} &= \mu\mathcal{E}_0 e^{i\Delta(t)t} \gamma_I \end{aligned} \quad (11)$$

While Equation (11) is not directly solvable, as an approximation, one could solve for when $\Delta(t)$ as a constant, and then re-introduce $\Delta(t)$ as a function of time. This procedure produces a modified form of Rabi's formula, as shown in Equation (12), when solved with the initial condition $\gamma_I = 1$.

$$\begin{aligned} P_I &= |\gamma_I|^2 = 1 - \frac{\mu^2 \mathcal{E}_0^2 / \hbar^2}{\mu^2 \mathcal{E}_0^2 / \hbar^2 + (\Delta(t))^2 / 4} \sin^2 \left(\sqrt{\frac{\mu^2 \mathcal{E}_0^2}{\hbar^2} + \frac{(\Delta(t))^2}{4}} t \right) \\ P_{II} &= |\gamma_{II}|^2 = \frac{\mu^2 \mathcal{E}_0^2 / \hbar^2}{\mu^2 \mathcal{E}_0^2 / \hbar^2 + (\Delta(t))^2 / 4} \sin^2 \left(\sqrt{\frac{\mu^2 \mathcal{E}_0^2}{\hbar^2} + \frac{(\Delta(t))^2}{4}} t \right) \end{aligned} \quad (12)$$

A. Comparison with Numerical Solution

To verify the approximations thus far in Equation (12), it can be compared with numerical solutions of Equation (7). The approximations prior to Equation (7) are same as those used in the derivation of Rabi cycles, and have been experimentally verified and hence do not require additional justification [9]. The numerical solution uses the Matlab implementation of TR-BDF2 in the function ode23tb, chosen for the numerical stability which prevents total probability from increasing for long solutions [10]. The forcing function is of the form shown in Equation (13).

$$\begin{aligned} \mathcal{E} &= 2\mathcal{E}_0 \cos((\omega_0 + \Delta(t))t) \\ \Delta(t) &= \Delta' t \end{aligned} \quad (13)$$

The numerical results are shown in Figures 1, 2, and 3 together with plots of Equation (12). The value used for the resonant frequency (ω_0) is that of Ammonia inversion, chosen as the model system [11]. Similarly, the value of dipole moment (μ) used is that of ammonia [11]. It can be seen the approximation holds up well for one cycle, even though the probability diverges quickly afterwards. This suggests that the approximate formula in Equation (12) would work for characterization of frequency response based on peak population of the initially unpopulated state.

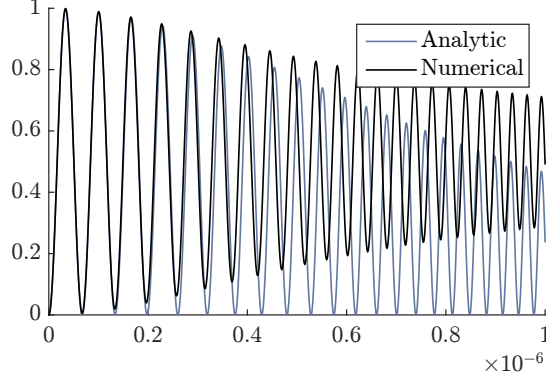


FIG. 1. Probability that the system is in state II as a function of t . Forcing is $2\mathcal{E}_0 \cos((w_0 + \Delta't)t)$, where $\omega_0 = 2\pi \times 23870$ Mhz, $w' = 1 \times 10^{14} \text{ s}^{-2}$, $\mu = 1.472 \text{ D}$, and $\mathcal{E}_0 = 1000 \text{ NC}^{-1}$.

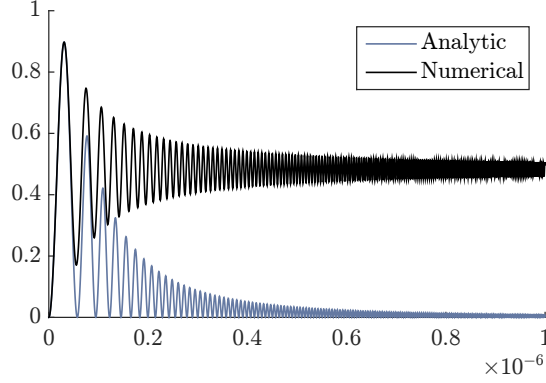


FIG. 2. Probability that the system is in state II as a function of t . Forcing is $2\mathcal{E}_0 \cos((w_0 + \Delta't)t)$, where $\omega_0 = 2\pi \times 23870$ Mhz, $w' = 1 \times 10^{15} \text{ s}^{-2}$, $\mu = 1.472 \text{ D}$, and $\mathcal{E}_0 = 1000 \text{ NC}^{-1}$.

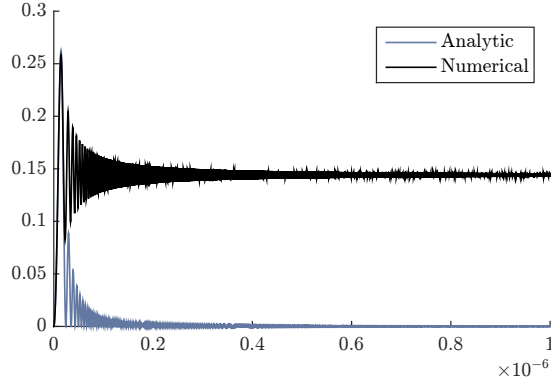


FIG. 3. Probability that the system is in state II as a function of t . Forcing is $2\mathcal{E}_0 \cos((w_0 + \Delta't)t)$, where $\omega_0 = 2\pi \times 23870$ Mhz, $w' = 1 \times 10^{16} \text{ s}^{-2}$, $\mu = 1.472 \text{ D}$, and $\mathcal{E}_0 = 1000 \text{ NC}^{-1}$.

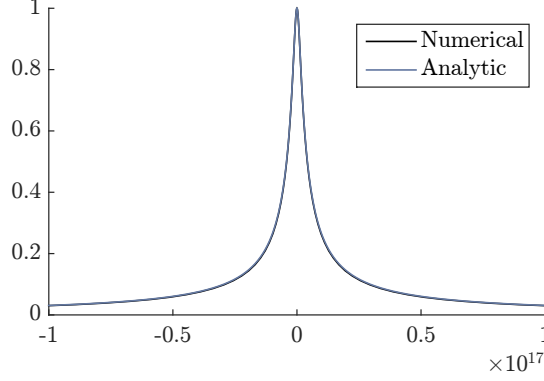


FIG. 4. Peak probability that the system is in state $|II\rangle$ as a function of w' . Forcing is $2\mathcal{E}_0 \cos((\omega_0 + \Delta't)t)$, where $\omega_0 = 2\pi \times 23870$ Mhz, and $\mathcal{E}_0 = 1000 \text{ NC}^{-1}$. The two lines are overlapping.

III. FREQUENCY RESPONSE TO CHIRP SIGNAL AS FORCING FUNCTION

To determine the frequency response, the peak population of the initially unpopulated state has to be determined. To do this one could find the zero of $\frac{dP_{II}}{dt}$, and then use that time-value to determine the probability at that point from Equation (12). The peak probability would be called P_{max} .

This would involve solving Equation (14). As it is a transcendental equation, the it would have to be solved numerically. This is done using the `fzero` function in Matlab.

$$\begin{aligned} & \frac{\Delta(t)\dot{\Delta}(t)}{2(\mu^2\mathcal{E}_0^2/\hbar^2 + (\Delta(t))^2/4)} \sin\left(\sqrt{\frac{\mu^2\mathcal{E}_0^2}{\hbar^2} + \frac{\Delta(t)^2}{4}} t\right) + \\ & 2\left(\sqrt{\frac{\mu^2\mathcal{E}_0^2}{\hbar^2} + \frac{\Delta(t)^2}{4}} + \frac{t\Delta(t)\dot{\Delta}(t)}{4\sqrt{\mu^2\mathcal{E}_0^2/\hbar^2 + (\Delta(t))^2/4}}\right) \cos\left(\sqrt{\frac{\mu^2\mathcal{E}_0^2}{\hbar^2} + \frac{\Delta(t)^2}{4}} t\right) = 0 \end{aligned} \quad (14)$$

For a linear chirp signal of the form shown in Equation (13), Figure 4 can be produced. It can be seen that the solution based on solution of Equation (14) is very similar to the solution obtained by numerically solving the differential equation Equation (8) and obtaining the peak value from that. This is because while Equation (12) is not the exact solution of Equation (11), the Hamiltonian changes slowly over the course of the first oscillation. Thus, Equation (12) can be considered an adiabatic approximation, up to the first transition. This does not work beyond the first oscillation, however, as errors are cumulative.

That allows us to construct the same same frequency response graph with a different value of \mathcal{E}_0 . The numerical solution is more expensive to compute with small values of \mathcal{E}_0 .

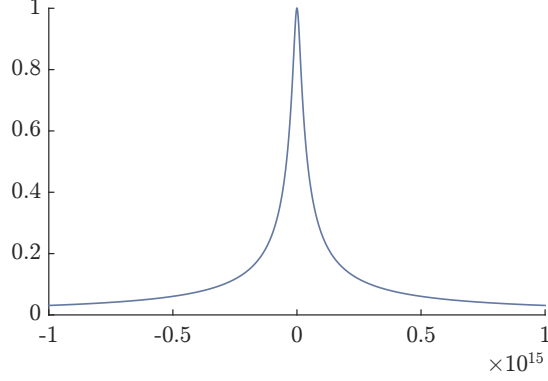


FIG. 5. Peak probability that the system is in state $|II\rangle$ as a function of w' . Forcing is $2\mathcal{E}_0 \cos((w_0 + \Delta't)t)$, where $\omega_0 = 2\pi \times 23870$ Mhz, and $\mathcal{E}_0 = 100 \text{ NC}^{-1}$.

as the Rabi flopping described by Equation (12) is slower even though the forcing frequency does not change, however the analytical method does not suffer from this limitation. This allows us to obtain Figure 5.

IV. DISCUSSION OF RESULTS

The main results are shown in Figure 4 and Figure 5. Figure 4 represents a solution with electric field strength of $\mathcal{E}_0 = 1000 \text{ NC}^{-1}$. That is a very high value, corresponding to dielectric heating power per volume of $7.23 \times 10^5 \text{ Wm}^{-3}$ of room temperature water, for $\epsilon'' = 10.62$ as the value of imaginary relative permittivity [12]. This value also corresponds to a plane wave Poynting vector magnitude of 1327 Wm^{-2} . This is comparable to the expected power density for microwave power transmission from space-based solar power [13].

Figure 5 represents a lower value, of $\mathcal{E}_0 = 100 \text{ NC}^{-1}$. This represents a plane wave Poynting vector magnitude of 13.27 Wm^{-2} , which is more typical of low power microwave power transmission for microelectronics [14].

It can be seen from the values obtained that the effect is not entirely simply due to the Δ' term changing the frequency to be far enough from resonance. Using the system parameters presented in Figure 3, the first peak in the population of the upper level occurs at $1.45 \times 10^{-8} \text{ s}$. At that time, $\Delta't = 1.45 \times 10^8 \text{ Hz}$. If this is taken as the static value of Δ in Equation (12), the resultant amplitude is 0.292, which is higher than the value in 3 of 0.258. Mathematically, this is due to the time dependence of $\Delta't$ resulting in the peak not

being in the same time coordinate as that of the original Rabi oscillation, necessitating a numerical solution of the transcendental equation (14).

A. Relation to Penetration Depth

One can determine the change in penetration depth with a few assumptions. The first assumption is that intensity of radiation in the material being investigated decays linearly; that is, attenuation is linear. The second assumption is that when a molecule is raised to a higher energy state due to rabi oscillations, it immediately relaxes to the ground state. This could be achieved by strong phonon couplings in a solid where the temperature k_bT is much lower than $\hbar\omega$, for example. The final assumption is that there is no anisotropy in the material. In such a scenario, the absorption would be described by Equation (15).

$$\frac{dI}{dz} = -\frac{I}{\lambda} \quad (15)$$

The above equation can be interpreted as a probability of absorption of photon, such that the probability of a photon being absorbed by a film of infinitesimal thickness δz is $\frac{\delta z}{\lambda}$. It follows from the above assumptions that if the peak population of the upper level is decreased from 1 to p , such that $0 < p < 1$, then the probability of a photon being absorbed by a film of infinitesimal thickness δz is $\frac{p\delta z}{\lambda}$. Thus, the new penetration depth is given by Equation (16), and has an inverse linear relationship to the peak probability of the Rabi oscillation at a certain chirp rate.

$$\lambda' = \frac{\lambda}{p} \quad (16)$$

B. Applications

As previously mentioned, one major application would be wireless power transfer, for both high power density transfer for long range transmission in the case of space-based solar, and low power density transmission for microelectronics. As the results in Figure 4 and Figure 5 show, the rate of frequency modulation required for significant reduction of peak population is much lower for a lower power signal. This implies that it would be significantly easier both experimentally verify and to utilize the result for low power density applications.

In addition to those applications, it is also possible to use a rapidly modulated signal as a carrier wave for communications [15]. This suggests that the same signal could be used for both power transfer and communications. Another advantage is that it is possible to use this fast frequency modulation as a form of multiplexing and to provide resistance to jamming, in a way similar to frequency-hopping spread spectrum [16].

Finally, as mentioned in the introduction, this has applications in the transmission of microwaves through dense media. It could enable wireless charging of and communications with embedded medical sensors or communications at greater depth with underwater craft.

C. Future and Related Work

Related work that has been done involved studying the effect of other types of nonlinear forcings, such as chaotic forcings, on 2-level quantum systems, and on classical oscillators. These results combined serve to enable wireless transmission of energy with EM waves while minimizing absorption by unintended sources, and minimizing unintended damage to organic material that crosses the field. Chaotic waves can also be used as carrier waves of communications [17, 18], hence the applications are similar to those of microwaves with fast frequency modulation as presented in this paper.

Future work could focus on the effect of nonlinear waves in the continuous spectra of a quantum system, or the construction of a proof-of-concept device to display the effects shown.

V. CONCLUSION

We presented results showing the peak population of a 2-level quantum system when perturbed by a chirp signal. It is shown using numerical solutions of Equation (8) that the peak population is reduced with a large chirp in Figure 4, and in the same figure this result is reproduced using a computationally cheaper procedure involving the solution of the transcendental equation shown in Equation (14). In addition, it is shown that the effect of a chirp signal in reducing peak population of the 2-level system is higher for weaker signals in Figure 5. This result has applications in wireless power transfer applications, both in potentially increasing overall system efficiency by decreasing unintended absorption by the

environment and in reducing the effect of wireless power transmission on organic tissue. However, it needs to be emphasized that this study does not directly address potential safety concerns of passing microwaves through live tissue and that further study is required.

The results based on two-level system presented can also be applied to quantum systems interacting with electromagnetic waves that are not described by merely two level Hamiltonians, as long as additional energy levels are much further from resonance and the rotating wave approximation holds, which requires weak coupling, where the Rabi frequency is much slower than the resonance frequency, which is the case in the results shown [19].

-
- [1] L. Liguang Xie, Y. Yi Shi, Y. T. Hou, and A. Lou, *IEEE Wireless Communications* **20**, 140 (2013).
 - [2] A. Sharma, V. Singh, T. L. Bougher, and B. A. Cola, *Nature Nanotechnology* **10**, 1027 (2015).
 - [3] P. Jaffe and J. McSpadden, *Proceedings of the IEEE* **101**, 1424 (2013).
 - [4] H. Takhedmit, L. Cirio, B. Merabet, B. Allard, F. Costa, C. Vollaie, and O. Picon, *Electronics Letters* **46**, 811 (2010).
 - [5] J. A. Tanner, *Nature* **210**, 636 (1966).
 - [6] K. Huang and X. Zhou, *IEEE Communications Magazine* **53**, 86 (2015).
 - [7] J. C. Reyes-Guerrero, M. Bokenfohr, and T. Ciamulski, in *WUWNET '14 Proceedings of the International Conference on Underwater Networks & Systems* (ACM Press, New York, New York, USA, 2014) pp. 1–2.
 - [8] A. Kovaleva and L. I. Manevitch, *Physical Review E* **88**, 024901 (2013).
 - [9] T. R. Gentile, B. J. Hughey, D. Kleppner, and T. W. Ducas, *Physical Review A* **40**, 5103 (1989).
 - [10] M. Hosea and L. Shampine, *Applied Numerical Mathematics* **20**, 21 (1996).
 - [11] P. Pracna, V. Špirko, and W. P. Kraemer, *Journal of Molecular Spectroscopy* **136**, 317 (1989).
 - [12] R. Buchner, J. Barthel, and J. Stauber, *Chemical Physics Letters* **306**, 57 (1999).
 - [13] S. Sasaki, K. Tanaka, and K. I. Maki, *Proceedings of the IEEE* **101**, 1438 (2013).
 - [14] N. Shinohara, *Proceedings of the 5th European Conference on Antennas and Propagation (EUCAP)*, 3970 (2011).
 - [15] A. Springer, W. Gugler, M. Huemer, L. Reindl, C. Ruppel, and R. Weigel, in *IEEE/AFCEA*

EUROCOMM 2000. Information Systems for Enhanced Public Safety and Security (Cat. No.00EX405) (IEEE, 2000) pp. 166–170.

- [16] L. Zhang, H. Wang, and T. Li, IEEE Transactions on Wireless Communications **12**, 70 (2013).
- [17] H. P. Ren, M. S. Baptista, and C. Grebogi, Physical Review Letters **110**, 184101 (2013).
- [18] J. C. Martín, Physical Review E **91**, 022914 (2015).
- [19] M. Frasca, “A modern review of the two-level approximation,” (2003), arXiv:0209056 [quant-ph].